Asymptotic solutions for turbulent mass transfer augmented by a first order chemical reaction

Maarten van Reeuwijk[a,*], Kaveh Sookhak Lari[b]

[a]*Department of Civil and Environmental Engineering, Imperial College London, London SW7 2AZ, UK.*
[b]*Department of Civil Engineering, University of Isfahan, Isfahan 81744-873441, Iran*

Abstract

We present asymptotic solutions for turbulent mass transfer in a smooth conduit at high Schmidt number in the presence of a first-order chemical reaction in the fluid. Exact far-field solutions are derived for a case dominated by 1) mass transfer at the wall and 2) the first-order chemical reaction. An approximate solution is derived for the regime where both are important. The solutions are in good agreement with numerical solutions and with the literature. At high Damköhler numbers the system is governed by a reaction-diffusion equation and the observed increase in mass transfer coefficient is caused by thinning of the mass transfer boundary layer due to the fast chemical reaction in the fluid. We present closed-form solutions for the far-field behaviour of Dirichlet, Neumann and Robin boundary conditions and comment on grid resolution requirements to accurately resolve the mass transfer boundary layer. The solution strategy presented can be straightforwardly extended to non-linear wall- and bulk-reactions.

Keywords: *Mass transfer; Turbulent wall-bounded flow; High Schmidt number; Asymptotic solution; bulk-reaction*

1. Introduction

Turbulent mass transfer in conduits is of relevance to a large number of engineering problems [1, 2]. Of particular interest is the determination of the mass transfer coefficient [3, 4, 5, 6, 7, 8], which allows for a direct calculation of the mass flux without a need to know details of the complex processes taking place in the fluid layer. In some situations, the mass transfer is augmented by a chemical reaction in the fluid, often referred to as a bulk-reaction. An example is the reaction of chlorine with natural organic matter which occurs during the transmission of drinking water [9, 10, 11]. The chemical reaction has the potential to significantly enhance the mass transfer coefficient [2, 12, 13, 14]. The aim of the present work is to provide closed-form solutions for this process and to understand in detail the physics behind this phenomenon.

A popular way to obtain predictions for mass transfer is to apply the method of separation of variables to the Reynolds-averaged mass-transport equation [15, 16, 17, 18]. This method transforms the partial differential equation (PDE) into an infinite series of ordinary differential equation (ODE) pairs each sharing a common eigenvalue. The eigenvalue problem can be solved straightforwardly, although the predictions are usually numerical because of the non-constant coefficients of the PDE. The solutions provide information both of the near-field where the concentration boundary layer is developing (and the mass transfer coefficient varies as a function of the streamwise coordinate), and the far-field where the concentration boundary layer is fully developed (mass transfer coefficient constant).

*Corresponding author. email: m.vanreeuwijk@imperial.ac.uk

If one is interested in the far-field behaviour only, it suffices to determine the lowest eigenvalue. Such a method was proposed by Sookhak Lari *et al.* [19], and has the advantage that it is straightforward to implement and fast to execute. Results were presented for a first-order wall reaction, i.e. a Robin boundary condition (BC) and a closed-form solution for concentration was developed. Garcia-Ybarra and Pinelli [20] arrived at the same closed-form solution using the method of matched asymptotic expansions for a Dirichlet BC. Sookhak Lari *et al.* later extended their work with a first order bulk reaction [21], and concluded that wall and bulk-reactions can be modelled independently, even at high Damköhler numbers (*Da*).

Recently, we generalized the work of Sookhak Lari *et al.* [19] and Garcia-Ybarra and Pinelli [20] to arbitrary BCs [22]. Key to the method was the large difference between the small lengthscales in the wall-normal direction and the large lengthscales in the streamwise direction. This allowed fast variations in the wall-normal direction to be solved independently from the slow variations in the streamwise direction, and led to asymptotic solutions both for linear and nonlinear BCs. An interesting finding was that the mass transfer coefficient k_{f0} $[LT^{-1}]$ is entirely independent of wall reaction type and given by [22]

$$k_{f0} = \frac{9}{2\pi\sqrt{3}}\left(\frac{b}{Sc_T}\right)^{1/3} Sc^{-2/3} u_\tau. \tag{1}$$

Here, the Schmidt number Sc represents the ratio of kinematic viscosity to molecular diffusivity and u_τ $[LT^{-1}]$ is the shear velocity. The parameter b represents a turbulence coefficient and Sc_T is the turbulence Schmidt number. The coefficient b can be inferred from the wall-normal variation in the eddy viscosity and is found to be close to 0.001 [6, 22, 2], although other

values are reported [6, 20, 23]. The coefficient Sc_T is approximately unity away from the wall, but is known to vary very close to the wall for high Sc compounds [23, 24, 25, 26, 27]. The implications on the present work will be discussed in §4 and §6.

In this paper, we extend the work of Van Reeuwijk and Sookhak Lari [22] by adding a chemical reaction taking place in the fluid (§2). First-order reactions will be considered here, but the method is equally applicable to nonlinear reactions (both in the bulk and on the wall). We present far-field solutions (§3) and discuss the enhancement of the mass transfer coefficient due to the presence of the bulk-reaction (§4). We calculate the decay coefficient for Dirichlet, Neumann and Robin BCs and compare the results with numerical solutions (§5). Concluding remarks are made in §6.

2. Governing equations

Consider the transport of a high Sc solute through a conduit at high Reynolds number Re which exchanges mass with the conduit walls and is subject to a first order chemical reaction with reaction coefficient k_b $[T^{-1}]$. For fully developed flow through a pipe with radius R, the governing equation is the axisymmetric Reynolds-averaged, steady-state mass transport equation [2]

$$u\frac{\partial C}{\partial x} - \frac{1}{r}\frac{\partial}{\partial r}\left[r\left(D + D_T\right)\frac{\partial C}{\partial r}\right] + k_b C = 0, \tag{2}$$

where x $[L]$ and r $[L]$ are the streamwise and radial directions, and $C(x,r)$ is the (Reynolds-averaged) mass concentration $[ML^{-3}]$. The velocity, molecular and eddy diffusivity are denoted by u $[LT^{-1}]$, D $[L^2T^{-1}]$ and D_T $[L^2T^{-1}]$, respectively. Streamwise diffusion has been neglected, as is common for these problems [18]. The axisymmetric coordinate system is used for convenience of presentation; the approach is equally valid for non-circular cross-sections as long as the viscous wall region is much thinner than the local surface curvature.

Equation (2) is supplemented by BCs of the form

$$C(x=0,r) = C_0 \tag{3}$$

$$\left.\frac{\partial C}{\partial r}\right|_w = G(C_w), \tag{4}$$

$$C(x, r=0) = C_b(x) \tag{5}$$

where C_0 is the initial concentration, $C_w = C(x,R)$, $\partial C/\partial r|_w = \partial C/\partial r(x,R)$ and $G(C_w)$ is a generic function which depends on the wall concentration. We note that (5) is an unusual BC; it is common to impose a Neumann BC on the centerline. However, the physics of this problem is such that the concentration in the bulk is constant which is why it will prove more convenient to impose (5) [20, 22].

Indeed, for high Sc mass transfer, the area of interest is a very thin layer of fluid immediately adjacent to the wall where concentration gradients are large [6, 20, 19, 21, 22], referred to as the mass transfer boundary layer (MTBL). Outside the MTBL, the concentration is approximately uniform. As the MTBL will be nested inside the viscous sublayer at high Sc, the velocity u and eddy diffusivity D_T can be characterised by

$$u^+ = y^+, \qquad \frac{D_T}{D} = b\frac{Sc}{Sc_T}y^{+3}, \tag{6}$$

where $u^+ = u/u_\tau$ and $y^+ = y/\delta_\nu$. Here, $u_\tau = \sqrt{\tau_w/\rho}$ $[LT^{-1}]$ is the shear velocity, τ_w $[ML^{-1}T^{-2}]$ is the wall shear stress, ρ $[ML^{-3}]$ is the fluid density, $\delta_\nu = \nu/u_\tau$ $[L]$ is the viscous lengthscale and ν $[L^2T^{-1}]$ is the kinematic viscosity. Equation (6) can be obtained with a Taylor series expansion [28, 2, 20] for a Dirichlet BC for concentration. For other concentration BCs, D_T may have a different leading order term [29] although it is currently unclear how influential this is. For a detailed discussion on this topic we refer to [22]. In this paper we will use the classical assumption that D_T is a cubic and that Sc_T is a constant [6, 2].

Using Eq (6), a typical MTBL thickness δ_{m0} can be defined as the distance from the wall where $D = D_T$, with result [6, 22]

$$\delta_{m0} = \sqrt[3]{\frac{Sc_T}{bSc}}\delta_\nu. \tag{7}$$

Here, it is noted that δ_{m0} is the MTBL thickness in absence of the chemical reaction in the fluid, which can make the MTBL thinner (see §3).

As the variations in concentration occur in the MTBL, a suitable change of variables is $x = \mathcal{L}\xi$ and $r = R - \delta_{m0}\eta$, where $\mathcal{L}$ is a yet unspecified lengthscale. Substitution of (6) in (2)-(5) then leads to

$$\epsilon\eta\frac{\partial C}{\partial \xi} - \frac{\partial}{\partial \eta}\left[\left(1+\eta^3\right)\frac{\partial C}{\partial \eta}\right] + \kappa^2 C = 0, \tag{8}$$

$$\left.\frac{\partial C}{\partial \eta}\right|_w = g(C_w), \tag{9}$$

$$C(\xi, \eta\to\infty) = C_b(\xi), \tag{10}$$

where $g(C_w) = \delta_{m0}G(C_w)$ and

$$\epsilon = \frac{Sc_T}{b}\frac{\delta_\nu}{\mathcal{L}} = \frac{2Sc_T}{b}\frac{r_h}{\mathcal{L}}Re_\tau^{-1}, \tag{11}$$

$$\kappa = \frac{k_b^{1/2}\delta_{m0}}{D^{1/2}} = \left(\frac{Sc_T}{b}\right)^{1/3} Da_\tau^{1/2} Sc^{1/6}. \tag{12}$$

Here, $r_h = R/2$ $[L]$ is the hydraulic radius, $Re_\tau = u_\tau R\nu^{-1}$ is the shear Reynolds number which represents the conduit size in plus-units and $Da_\tau = k_b\nu/u_\tau^2$ is the Damköhler number which represents the ratio of the viscous to the reaction timescale. The parameter ϵ expresses the ratio of near-field (entrance) lengthscale $Sc_T\delta_\nu/b$ [22] to far-field lengthscale $\mathcal{L}$, whilst κ represents the ratio of the lengthscale δ_{m0} to the diffusive lengthscale associated with the bulk reaction $(D/k_b)^{1/2}$.

The governing equation of the bulk concentration C_b can be obtained by averaging (2) over the cross-section:

$$\frac{\mathrm{d}}{\mathrm{d}x}\langle uC\rangle - \frac{D}{r_h}\left.\frac{\partial C}{\partial r}\right|_w + k_b\langle C\rangle = 0, \tag{13}$$

Here, $\langle C\rangle = \frac{2}{R^2}\int_0^R rC\,\mathrm{d}r$ and $\langle uC\rangle = \frac{2}{R^2}\int_0^R ruC\,\mathrm{d}r$ are the average concentration and streamwise mass flux, respectively. Because C is constant throughout the cross-section except in the MTBL for the problem under consideration, $\langle uC\rangle \approx UC_b$ and $\langle C\rangle \approx C_b$, where $U = \langle u\rangle$ is the average velocity. This results in

$$U\frac{\mathrm{d}C_b}{\mathrm{d}x} + \frac{J_w}{r_h} + k_b C_b = 0, \tag{14}$$

where J_w is the wall mass flux per unit area $[MT^{-1}L^{-2}]$:

$$J_w = -D\left.\frac{\partial C}{\partial r}\right|_w = \frac{D}{\delta_{m0}}\left.\frac{\partial C}{\partial \eta}\right|_w. \tag{15}$$

Substituting (15) into (14) and a change of coordinates $x = \mathcal{L}\xi$ results in

$$\frac{\mathrm{d}C_b}{\mathrm{d}\xi} + \frac{D\mathcal{L}}{\delta_{m0} r_h U}\left.\frac{\partial C}{\partial \eta}\right|_w + \frac{k_b\mathcal{L}}{U}C_b = 0. \tag{16}$$

The equation above provides guidance on how to define the typical streamwise lengthscale $\mathcal{L}$. Depending on whether the wall reaction or the bulk reaction dominates, $\mathcal{L}$ will take a different form. If bulk-reactions are negligible, $\mathcal{L}/r_h \approx \delta_{m0}U/D$. When bulk-reactions dominate, $\mathcal{L}/r_h \approx U/k_b r_h$. Hence, it is impossible to define one simple parameter group which captures the behaviour in both limits.

A definition of $\mathcal{L}$ which picks up the correct limiting behaviour in both situations is

$$\frac{\mathcal{L}}{r_h} = \left(\frac{k_b r_h}{U} + \frac{D}{U\delta_{m0}}\right)^{-1}. \tag{17}$$

Using (1), we can rewrite (17) as

$$\frac{\mathcal{L}}{r_h} = \left(Da + \frac{2\pi\sqrt{3}}{9}St\right)^{-1}, \tag{18}$$

where $Da = k_b r_h/U$ is the bulk Damköhler number and $St = k_{f0}/U$ is the bulk Stanton number.

Using (18), equation (16) becomes

$$\frac{\mathrm{d}C_b}{\mathrm{d}\xi} + (1-\Omega)\left.\frac{\partial C}{\partial \eta}\right|_w + \Omega C_b = 0, \tag{19}$$

where

$$\Omega = \frac{Da}{Da + 2\pi\sqrt{3}St/9} \tag{20}$$

is a parameter representing the importance of the bulk-reactions. If $\Omega \approx 0$, the problem is dominated by mass transfer at the wall, and if $\Omega \approx 1$ the problem is dominated by the first-order bulk-reaction.

3. Far-field solutions for concentration

Equation (8) is a singular perturbation problem involving two small parameters ϵ and δ_{m0}/R, the former associated with entrance effects and the latter with the extremely thin MTBL. The parameter δ_{m0}/R is not visible in (8) because this equation is written in terms of the inner variable η.

We will assume that ϵ is so small that the advective term can be neglected, which effectively means restricting attention to the far-field. Substituting (18) into (11) results in

$$\epsilon = \frac{2Sc_T}{b}\left(\frac{Da}{Re_\tau} + \frac{2\pi\sqrt{3}}{9}\frac{St}{Re_\tau}\right). \tag{21}$$

Requiring that $\epsilon < 10^{-3}$ and assuming that $Re_\tau = 1000$, the equation above implies $Da < O(10^{-3})$ and $St < O(10^{-3})$. These restrictions are satisfied in many applications [12, 20, 21, 22]. The problem then simplifies to

$$-\frac{\partial}{\partial\eta}\left[\left(1+\eta^3\right)\frac{\partial C}{\partial\eta}\right] + \kappa^2 C = 0, \tag{22}$$

which is a classical boundary layer problem that can be solved using matched asymptotic expansions [30]. This approach was pursued by Garcia-Ybarra and Pinelli [20] who derived a solution to the problem for $\kappa = 0$. They found that the outer solution is trivial: the concentration is constant. This was further confirmed by van Reeuwijk and Sookhak Lari [22] who performed a detailed comparison between the asymptotic solution and a numerical approximation of (2). As the only nontrivial behaviour in C takes place within a few inner units [20, 22], it suffices to study (22) in inner variables only and no asymptotic matching is necessary.

Because the differential operators in (22) are in terms of η only, this equation can be solved independently from the ξ direction, and the ξ dependence will only enter the solution via the integration constants. Below, we will present closed-form solutions for $\kappa \ll 1$, $\kappa \gg 1$ and an approximate solution for intermediate κ.

3.1. $\kappa \ll 1$

Upon assuming $\kappa \ll 1$, (22), (9) and (10) reduce to the system considered by Van Reeuwijk and Sookhak Lari [22]; the solution is given by

$$C(\xi,\eta) = C_b + (C_b - C_w)F(\eta), \tag{23}$$

where $F(\eta)$ is defined as

$$F(\eta) = \frac{\sqrt{3}}{2\pi}\left(\log\frac{\eta+1}{\sqrt{\eta^2-\eta+1}} - \sqrt{3}\left(\frac{\pi}{2} - \arctan\frac{2\eta-1}{\sqrt{3}}\right)\right). \tag{24}$$

The function F increases monotonically from $F(0) = -1$ to $F(\infty) = 0$.

3.2. $\kappa \gg 1$

When $\kappa \gg 1$, the diffusive lengthscale associated with the bulk reaction $(Dk_b^{-1})^{1/2}$ will be smaller than δ_{m0}. Consequently, the MTBL will become thinner and therefore turbulence will become less important. This can be made explicit by the change of variables $\eta_b = \eta/\kappa$, which transforms (22) in

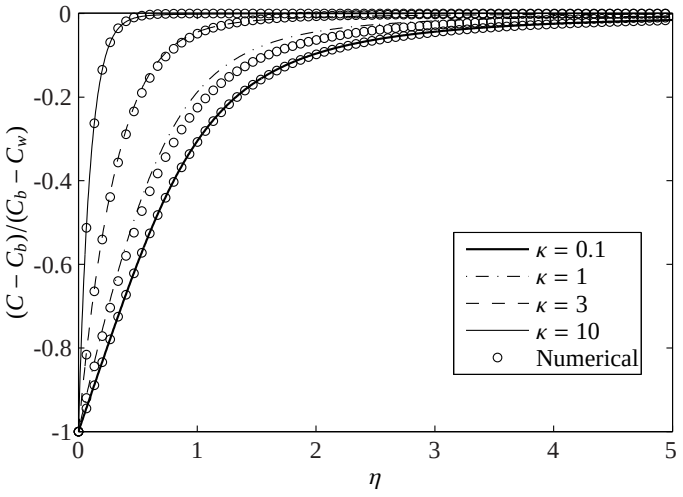

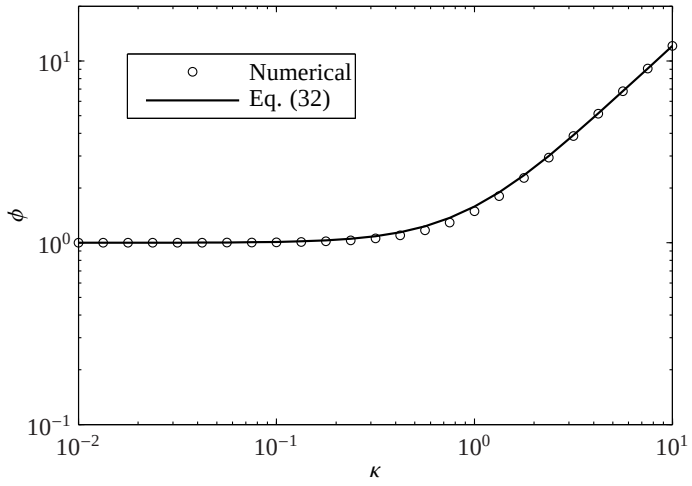

Figure 1: (a) C as a function of η for various κ. Eq. (29) (lines) and numerical solution to Eq. (22) (circles). (b) ϕ as a function of κ. Eq. (32) (thick solid line) and numerical solution to Eq. (22) (circles).

$$-\frac{\partial}{\partial \eta_b}\left[\left(1+\left(\frac{\eta_b}{\kappa}\right)^3\right)\frac{\partial C}{\partial \eta_b}\right] + C = 0. \tag{25}$$

In the limit of $\kappa \to \infty$, the equation above confirms that turbulence does not play a role and the system behaves as a classical reaction-diffusion problem. The general solution is then given by

$$C = A_1 \exp(-\eta_b) + A_2 \exp(\eta_b), \tag{26}$$

where A_1 and A_2 are constants determined by the BCs. The only permissible BCs are $A_1 = C_w$ and $A_2 = 0$, the latter implying that $C_b = 0$. From a physical perspective this is understandable, because the reactions are so fast that there is no remaining solute mass in the bulk. In terms of η, the solution is therefore given by

$$C = C_w \exp(-\kappa\eta). \tag{27}$$

3.3. Intermediate κ

We were unable to obtain closed-form solutions to equation (22). However, an approximation can be obtained by noticing that the second term of (22) is only important for large κ. Therefore, (27) is substituted into the second term which results in

$$-\frac{\partial}{\partial \eta}\left[(1+\eta^3)\frac{\partial C}{\partial \eta}\right] + C_w\kappa^2 \exp(-\kappa\eta) = 0. \tag{28}$$

This approach follows [12] where it was successfully used to create an approximate correlation for k_f. The solution to Eq. (28) is given by

$$C(\xi,\eta) = C_b + (C_b - C_w)F(\eta) - C_w\left[B(\eta;\kappa) - B(\infty;\kappa)(F(\eta)+1)\right], \tag{29}$$

where

$$B(\eta;\kappa) = \sum_{m=1}^{3} \frac{\kappa z_m \exp(-\kappa z_m)}{3}\left(E_1\left(\kappa(\eta - z_m)\right) - E_1\left(-\kappa z_m\right)\right). \tag{30}$$

Here, E_1 is the exponential integral [31], $z_m = \exp(i\theta_m)$, $\theta_m = (2m-1)\pi/3$ and $i^2 = -1$. Note that B is a real function because $z_1 = \overline{z}_3$ and $E_1(\overline{z}) = \overline{E_1(z)}$ where the overline denotes the complex conjugate. Note that $B(\infty;\kappa = 0) = 0$ and $B(\infty;\kappa = \infty) = 1$.

Figure 1(a) shows concentration profiles as a function of η for various κ (lines). The BCs used were $C_w = 1$ and $C_b = 0$, the former having no influence on the figure and the second a necessity because $C_b = 0$ in the far-field for $\kappa \gg 1$. For $\kappa \ll 1$, the solution is equal to $F(\eta)$ defined in (24) (thick black line). As κ becomes larger, the diffusive reaction lengthscale $(D/k_b)^{1/2}$ becomes smaller than δ_{m0}, resulting in a thinner MTBL.

In order to determine the appropriateness of the approximate analytical solution (29) the results are compared to numerical solutions of (22). The numerical integration is performed with a Runge-Kutta 4/5th scheme, and a shooting method is used to enforce the zero concentration in the center of the conduit. By decreasing the tolerance, it was confirmed that the solutions presented here are fully converged.

Figure 1(a) demonstrates that the approximate solution (29) (lines) matches excellently with the numerical solution of (22) for $\kappa \ll 1$ and $\kappa \gg 1$, which is no surprise because the solution is exact in these limits. At $\kappa = O(1)$ the approximation is less accurate but still acceptable.

4. The enhancement factor

The mass transfer coefficient k_f can be found by substituting (29) into (15) and plugging the result into the definition $k_f = J_w/(C_b - C_w)$ which results in

$$k_f = \left[\frac{9}{2\pi\sqrt{3}} - \frac{C_w}{C_b - C_w}\left(\kappa - \frac{9B(\infty;\kappa)}{2\pi\sqrt{3}}\right)\right]\frac{D}{\delta_{m0}}. \tag{31}$$

The second term will only be important if κ is large, for which $C_b \approx 0$ and therefore $C_w/(C_b - C_w) \approx -1$. It is interesting to note that as opposed to (1), (31) is not strictly universal, in the sense that it requires BC information through the term C_w. This is a result of the consumption of solute mass in the MTBL. For $\kappa \ll 1$, k_f is consistent with (1). For $\kappa \gg 1$, we find that $k_f \approx (k_b D)^{1/2} = Da_\tau^{1/2} Sc^{-1/2} u_\tau$.

The enhancement factor ϕ which is defined as $\phi = k_f/k_{f0}$ is given by

$$\phi = \left[1 - \frac{C_w}{C_b - C_w}\left(\frac{2\pi\sqrt{3}}{9}\kappa - B(\infty;\kappa)\right)\right]. \qquad (32)$$

Figure 1(b) demonstrates that Eq. (32) (thick solid line) is in good agreement with the numerical solutions (circles). Both limits $\kappa \ll 1$ and $\kappa \gg 1$ are captured correctly, and the cross-over from one regime to the other is picked up well. The maximum difference in ϕ between (32) and the numerical solution is 7 percent.

Figure 2 shows a comparison of (32) (solid line) with the theoretical correlation proposed by Hanna *et al.* [12] (triangles):

$$\phi_{HSW} = \left[1 + \left(\frac{\kappa}{0.827}\right)^2\right]^{1/2}. \qquad (33)$$

Here we note that their α is simply the square of κ. The two correlations are practically indistinguishable, which is not entirely surprising as both approaches are theoretical and make similar assumptions.

Also shown in Figure 2 is the correlation proposed by Mitrovic and Papavassiliou [13] (dash-dotted lines)

$$\phi_{MP} = \left[1 + (0.74 Sc^{0.11}\kappa)^{2.4}\right]^{1/3} \qquad (34)$$

for various Sc. This correlation was obtained from a fit to data obtained using classical Eulerian Direct Numerical Simulation (DNS) for the flow and a Lagrangian method to simulate the mass transfer. Two main differences between ϕ and ϕ_{MP} can be observed: 1) the cross-over point κ_c between the two regimes is a function of Sc for ϕ_{MP}, and 2) the slopes of ϕ and ϕ_{MP} are different at high κ. We define the cross-over point κ_c as the value for κ for which the term of ϕ involving κ takes the value 1. For ϕ_{HSW} this occurs at $\kappa_c = 0.827$ (no Sc dependence) and for ϕ_{MP} this occurs at $\kappa_c = 1.35 Sc^{-0.11}$. For ϕ, a root finding algorithm is required which results in $\kappa_c = 1.439$.

The first difference, the Sc dependence of the cross-over point, may be explained by noting that the present work does not take into consideration that Sc_T is not constant very close to the wall and is also dependent on Sc [23, 24, 25, 26, 27]. The variation in Sc_T implies that the assumed cubic behaviour of D_T in (6) may not be representative for the entire diffusive sublayer [26, 29]. This will directly influence the mass-transfer characteristics of the MTBL. In the context of ϕ, these effects will introduce a new Sc dependence in the boundary layer thickness δ_{m0} which will in turn influence the cross-over from the mass-transfer regime to the reaction-regime. Indeed, results from DNS obtained by Schwertfirm and Manhart [26] indicate that $\delta_{m0} \propto Sc^{-0.29}$, which when compared to (7) implies

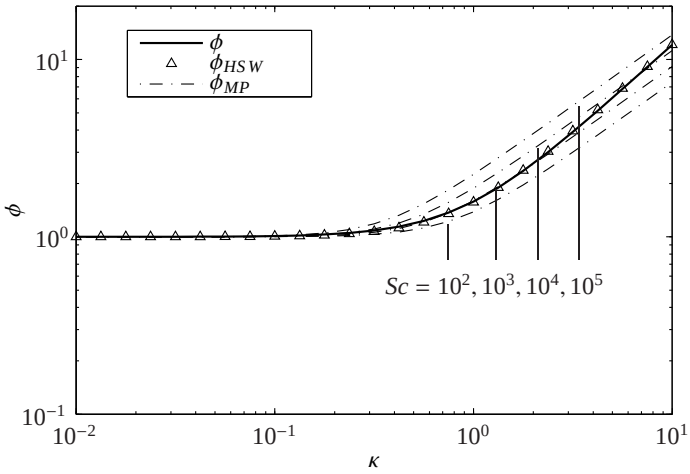

Figure 2: ϕ as a function of κ. Eq. (32) (thick solid line); Eq. (33) (Hanna *et al.*, triangles) and Eq. (34) for various Sc (Mitrovic and Papavassiliou, dash-dotted lines).

that $b/Sc_T \propto Sc^{-0.13}$. Substituting this into (12) shows that the cross-over point is then expected to vary as $\kappa_c \propto Sc^{-0.04}$, which is weaker than $\kappa_c \propto Sc^{-0.11}$ for ϕ_{MP} but has the correct trend.

The second difference, the difference in slope between ϕ and ϕ_{MP} for high κ is not so straightforward to pinpoint. Mitrovic and Papavassiliou [13] explain that for $\kappa \gg 1$ most Lagrangian markers will have reacted before they reach the so-called transition zone, which is the region where the particles are leaking away from the compact cloud of markers in the diffusive sublayer [32]. Our analysis confirms that this is indeed the case: for $\kappa \gg 1$ the governing equation is a reaction-diffusion equation and (32) shows that that $\phi \propto \kappa$ in that case. However, the DNS correlation (34) suggests that $\phi_{MP} \propto \kappa^{0.8}$ at high κ. It might be the case that the high κ results in [13] were influenced by numerics, perhaps because of the extremely thin MTBL at high Sc.

5. Far-field solutions for Dirichlet, Neumann and Robin BCs

Asymptotic solutions for Dirichlet, Neumann and Robin BCs can be derived by considering the linear BC

$$\alpha C_w + \beta \left.\frac{\partial C}{\partial \eta}\right|_w = \gamma, \qquad (35)$$

where α, β and γ are constants. By differentiating (24), we obtain

$$C_w = C_b - \frac{2\pi\sqrt{3}}{9} g(C_w). \qquad (36)$$

Using Eqs (9), (35) and (36), the wall concentration and gradient are given by

$$C_w = \frac{\beta C_b - 2\pi\sqrt{3}\gamma/9}{\beta - 2\pi\sqrt{3}\alpha/9}, \qquad \left.\frac{\partial C}{\partial \eta}\right|_w = \frac{\gamma}{\beta} - \frac{\alpha}{\beta} C_w. \qquad (37)$$

Substituting (37) into (19), solving for C_b and making use of (3) results in

$$C_b = \frac{A}{k} + \left(C_0 - \frac{A}{k}\right)\exp\left(-k\xi\right), \tag{38}$$

where

$$A = \frac{\gamma}{-\beta + 2\pi\sqrt{3}\alpha/9}(1-\Omega), \tag{39}$$

$$k = \Omega + (1-\Omega)\frac{\alpha}{-\beta + 2\pi\sqrt{3}\alpha/9}. \tag{40}$$

Shown in Figure 3 is the decay coefficient k for a Robin BC ($\alpha = -\sigma$, $\beta = 1$, $\gamma = 0$). The parameter σ is representative for the wall reaction speed. The Robin BC was chosen because it reproduces the behaviour of a Neumann BC for $\sigma \ll 1$ and a Dirichlet BC for $\sigma \gg 1$. Figure 3(a) shows the dependence of k on σ. In absence of bulk-reactions ($\Omega = 0$), k is linearly dependent on σ, whilst for large σ saturation occurs because of the finite conductivity of the MTBL [19, 22]. For nonzero Ω, a cross-over can be observed between a constant k if the problem is dominated by bulk-reactions,and an increasing k if the problem is dominated by wall-reactions [21]. Figure 3(b) shows k as a function of Ω. for $\sigma \ll 1$ (i.e. a Neumann BC), $k \approx \Omega$. For $\sigma \gg 1$ (i.e. a Dirichlet BC), $k \approx \Omega + 9(1-\Omega)/(2\pi\sqrt{3})$.

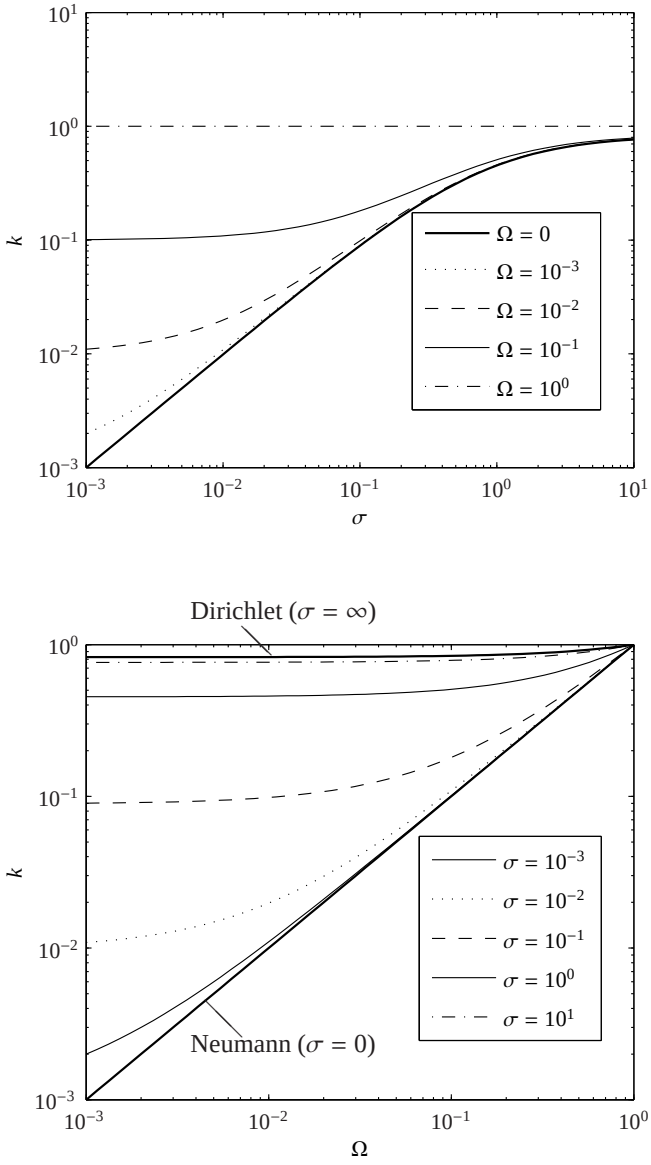

Figure 3: (a) Decay coefficient k as a function of σ for various Ω. (b) k as a function of Ω for various σ.

6. Concluding remarks

This paper presented closed-form asymptotic solutions for turbulent mass transfer in the presence of a first-order bulk-reaction. Two dimensionless groups were identified: ϵ which was the ratio of entrance lengthscale to far-field lengthscale, and κ which was the ratio of diffusive reaction lengthscale to MTBL thickness in absence of wall-reactions. Exact far-field solutions were presented for $\kappa \ll 1$ and $\kappa \gg 1$, and an approximate solution was presented for intermediate κ.

The enhancement factor ϕ was in good agreement with numerical solutions and also with the theoretical approximation ϕ_{HSW} developed by Hanna *et al.* [12] over the entire range of κ. As the approximation ϕ_{HWS} is much simpler to implement than ours but has similar accuracy, equation (33) is preferable for mass transfer calculations.

A comparison with the DNS correlation ϕ_{MP} of Mitrovic and Papavassiliou [13] highlights that the present work can be improved by improving the assumed profile for D_T. Indeed, spatial and Sc-dependent variations in Sc_T , which influence the boundary layer thickness δ_{m0}, were not taken into account in the present work. A dimensional argument showed that including this variation produced qualitatively the same behaviour as observed in (34). However, we were unable to explain the difference in slope between ϕ and ϕ_{MP} at very high κ, for which the problem reduces to a reaction-diffusion equation which has an exact solution.

An important opportunity for future work is to quantify in detail the profile of D_T as a function of Re_τ and Sc, using laboratory experiments or DNS. These results could then be

straightforwardly incorporated into the present method by letting b/Sc_T become an effective mass-transfer "conductivity" parameter. The calculation is explained in Ref. [22] Appendix A and involves mapping the profile of D_T onto a cubic under the restriction that the profiles are equally "conductive". The net effect of this procedure is that b/Sc_T becomes a parameter with a functional dependence on Sc and Re_τ.

The solutions presented here are valid for $Da < 10^{-3}$ and $St < 10^{-3}$, if $\epsilon = 10^{-3}$ is accepted as an upper bound in (21). For higher ϵ it will become necessary to resort to more sophisticated techniques, as 1) the separation of scales assumed in the present work will no longer be valid and 2) the assumption of uniform concentration in the bulk will cease to hold [19]. Within the range of applicability, the solution strategy presented here can be straightforwardly extended to non-linear wall- and bulk-reactions.

A practical aspect of the current work is that it provides guidance for the design of grids. Using (31) and (32) it follows that the MTBL thickness $\delta_m = \phi^{-1}\delta_{m0}$. Using approximation (33) and assuming $b/Sc_T = 0.001$ the expected MTBL thickness in plus-units is therefore

$$\delta_m^+ \approx 10Sc^{-1/3}\left[1+\left(\frac{\kappa}{0.827}\right)^2\right]^{-1/2} \tag{41}$$

There should be several grid-points in the MTBL. Note that for high κ, the horizontal resolution can be much lower that the wall-normal resolution because the problem then essentially reduces to a one-dimensional reaction-diffusion problem.

[1] J. Welty, C. Wicks, R. Wilson, G. Rorrer, Fundamentals of Momentum, Heat, and Mass transfer, John Wiley & Sons, Inc., New York, 2008.

[2] R. Bird, W. Stewart, E. Lightfoot, Transport Phenomena 2nd Ed., John Wiley and Sons, 2002.

[3] R. H. Notter, C. A. Sleicher, Solution to turbulent Graetz problem. 3. fully developed and entry region heat-transfer rates, Chem. Eng. Sci. 27 (1972) 2073.

[4] D. Shaw, Hanratty, Turbulent mass transfer rates to a wall at high Schmidt number, AlChE J. 23 (1977) 28–37.

[5] F. P. Berger, K. F. F. L. Hau, Mass-transfer in turbulent pipe-flow measured by electrochemical method, Int. J. Heat Mass Tran. 20 (1977) 1185–1194.

[6] B. A. Kader, Temperature and concentration profiles in fully turbulent boundary-layers, Int. J. Heat Mass Tran. 24 (1981) 1541–1544.

[7] W. Zhao, O. Trass, Electrochemical mass transfer measurements in rough surface pipe flow: geometrically similar V-shape grooves, Int. J. Heat Mass Tran. 40 (1997) 2785–2797.

[8] S. Aravinth, Prediction of heat and mass transfer for fully developed turbulent fluid flow through tubes, Int. J. Heat Mass Tran. 43 (2000) 1399–1408.

[9] L. A. Rossman, R. M. Clark, W. Grayman, Modelling chlorine residuals in drinking water distribution systems, J. Environ. Eng.-ASCE 120 (1994) 803–820.

[10] J. Crittenden, R. Trussell, D. Hand, K. Howe, G. Tchobanoglous, Water treatment principles and design, John Wiley & Sons, Inc., New York, 2005.

[11] L. Rossman, The effect of advanced treatment on chlorine decay in metallic pipes, Water Res. 40 (2006) 2493–2502.

[12] O. T. Hanna, O. C. Sandall, C. L. Wilson, Mass transfer accompanied by first-order chemical reaction for turbulent duct flow, Ind. Eng. Chem. Res. 26 (1987) 2286–2290.

[13] B. M. Mitrovic, D. V. Papavassiliou, Effects of a first-order chemical reaction on turbulent mass transfer, Int. J. Heat Mass Tran. 47 (2004) 43–61.

[14] C. A. Ramirez, Mass transfer enhancement by chemical reaction in turbulent tube flow, Chem. Eng. J. 138 (2008) 628–633.

[15] C. A. Sleicher, R. H. Notter, M. D. Crippen, A solution to turbulent Graetz problem by matched asymptotic expansions. 1. case of uniform wall temperature, Chem. Eng. Sci. 25 (1970) 845.

[16] P. Biswas, C. Lu, R. Clark, A model for chlorine concentration decay in pipes, Water Res. 27 (1993) 1715–1724.

[17] B. Weigand, M. Kanzamar, H. Beer, The extended Graetz problem with piecewise constant wall heat flux for pipe and channel flows, Int. J. Heat Mass Tran. 44 (2001) 3941–3952.

[18] B. Weigand, Analytical Methods for Heat Transfer and Fluid Flow Problems, Springer, 2004.

[19] K. Sookhak Lari, M. van Reeuwijk, C. Maksimović, Simplified numerical and analytical approach for solutes in turbulent flow reacting with smooth pipe walls, J. Hydraul. Eng.-ASCE 136 (2010) 626–632.

[20] P. I. Garcia-Ybarra, A. Pinelli, Turbulent channel flow concentration profile and wall deposition of a large Schmidt number passive scalar, C. R. Mechanique 334 (2006) 531–538.

[21] K. Sookhak Lari, M. van Reeuwijk, Č. Maksimović, S. Sharifan, Combined bulk and wall reactions in turbulent pipe flow: decay coefficients and concentration profiles, J. Hydroinform. 13 (2011) 324–333.

[22] M. van Reeuwijk, K. Sookhak Lari, Asymptotic solutions for turbulent mass transfer at high Schmidt number, Proc. R. Soc. A 468 (2012) 1676–1695.

[23] Y. Na, T. J. Hanratty, Limiting behavior of turbulent scalar transport close to a wall, Int. J. Heat Mass Tran. 43 (2000) 1749–1758.

[24] J. P. Crimaldi, J. R. Kossef, S. G. Monismith, A mixing-length formulation for the turbulent Prandtl number in wall-bounded flows with bed roughness and elevated scalar sources, Phys. Fluids 18 (2006) 095102.

[25] R. Bergant, I. Tiselj, Near-wall passive scalar transport at high Prandtl numbers, Phys. Fluids 19 (2007) 065105.

[26] F. Schwertfirm, M. Manhart, DNS of passive scalar transport in turbulent channel flow at high Schmidt numbers, Int. J. Heat Fluid Fl. 28 (2007) 1204–1214.

[27] M. Kozuka, Y. Seki, H. Kawamura, DNS of turbulent heat transfer in a channel flow with a high spatial resolution, Int. J. Heat Fluid Fl. 30 (2009) 514–524.

[28] R. A. Antonia, J. Kim, Turbulent Prandtl number in the near-wall region of a turbulent channel flow, Int. J. Heat Mass Tran. 34 (1991) 1905–1908.

[29] P. L. Garcia-Ybarra, Near-wall turbulent transport of large-Schmidt-number passive scalars, Phys. Rev. E 79 (2009) 067302.

[30] M. van Dyke, Perturbation methods in fluid mechanics, The parabolic press, 1975.

[31] M. Abramowitz, I. Stegun (Eds.), Handbook of Mathematical Functions, Dover, 1970.

[32] D. V. Papavassiliou, Scalar dispersion from an instantaneous line source at the wall of a turbulent channel for medium and high Prandtl number fluids, Int. J. Heat Mass Tran. 23 (2002) 161–172.